Electron Dynamics of Passivated Gold Nanocrystals Probed by Subpicosecond Transient Absorption Spectroscopy

S. L. Logunov, T. S. Ahmadi, and M. A. El-Sayed*

School of Chemistry and Biochemistry, Georgia Institute of Technology, Atlanta, Georgia 30332-0400

J. T. Khoury and R. L. Whetten

School of Physics & Chemistry, Georgia Institute of Technology, Atlanta, Georgia 30332-0430

Received: September 23, 1996; In Final Form: January 8, 1997[⊗]

The electronic dynamics of gold nanocrystals, passivated by a monolayer of alkylthiol(ate) groups, were studied by transient spectroscopy after excitation with subpicosecond laser pulses. Three solution-phase gold samples with average particle size of 1.9, 2.6, and 3.2 nm with size distribution less than 10% were used. The photoexcitation in the intraband (surface plasmon region) leads to the heating of the conduction electron gas and its subsequent thermalization through electron−electron and electron−phonon interaction. The results are analyzed in terms of the contribution of the equilibrated "hot" electrons to the surface plasmon resonance of gold. A different spectral response was observed for different sizes of gold nanoparticles. The results were compared to the dynamics of the large (30 nm diameter) gold nanocrystals colloidal solution. The size-dependent spectral changes are attributed to the reduction of the density of states for small nanoparticles. The observed variation in the kinetics of the cooling process in gold nanoparticles with changing the laser intensity is attributed to the temperature dependence of the heat capacity of the electron gas.

Introduction

The existence of free carriers in metallic nanoparticles gives rise to many interesting linear and nonlinear optical properties that have been extensively studied.[1] Investigations involving the interactions of free carriers among themselves and their environment are especially significant in solid state physics.[2] An understanding of the electron−phonon interactions is essential in the area of electrical and thermal transport in metals. Electron−electron interactions play an important role in disordered metallic systems.[3] A study of these phenomena in nanometer-scale metal particles may elucidate the evolution of these properties as a function of particle size.

In metallic nanoparticles, due to their small size and high surface-to-volume ratio, new optical properties arise which are observed neither in molecules nor in bulk metals. A particular example is the presence of a strong band in the visible region of the absorbance spectrum of noble metallic particles. This absorption band is attributed to surface plasmon oscillation modes of the conduction electrons in the particles which are coupled through the surface to the external applied electromagnetic field. Due to the presence of this plasmon band, the optical properties of copper, silver, and gold (more than others) colloidal nanoparticles have received considerable attention.[4−11] Mie[12] was the first to calculate the absorption spectrum of small gold particles using classical electromagnetic theory and the optical properties of bulk gold.

Recently, the possibility of generating transient nonequilibrium electron distributions in metals using ultrashort laser pulses has been explored. Methods such as thermal-assisted multiphoton photoemission,[13] single-photon photoemission,[14] and thermomodulation reflection and transmission[15−19] were employed in the study of nonequilibrium heating of electrons in thin metal films. At the ordinary temperatures, electronic heat capacity is much smaller than the lattice heat capacity; therefore, one can selectively excite the electron gas of metals and then monitor the electron thermalization dynamics in real time by various spectroscopic methods.[3] The small electronic heat capacity permits temperatures of thousands of degrees to be generated for durations up to a few picoseconds following an ultrashort laser pulse excitation.[17] Because of the high concentration of electrons in metals, it was assumed that thermal relaxation of the electron gas through electron−electron interactions would be instantaneous.[2] In the low radiation intensity limit, an electronic temperature change of ∼20 K was observed by Sun et al.[2] in gold thin films using transmission and reflection spectroscopy with infrared (pump) and visible (probe) femtosecond pulses. They found evidence for the transient non-Fermi electronic distribution with an electron thermalization time of ∼500 fs and an electron−phonon relaxation time of 1 ps.[2] However, the existence of nonequilibrium (non-Fermi) electron distributions with thermalization times of as long as 600 fs have been observed in thin gold films at higher excitation densities as well, i.e., electronic temperature changes of ∼400 K.[14,21]

The femtosecond dynamics of silver nanoparticles have been studied by exciting the plasmon band of the colloids at 390 nm.[6] It was suggested on the basis of the broad-band absorption around 750 nm that photoexcited electrons may form solvated electrons in the solid−liquid interface and relax through channels such as electron−phonon and phonon−solvent interactions. The time constants for the two processes were found to be 2 and 40 ps, respectively.

A recent study of the thermalization of electrons in copper nanoparticles embedded in glass using femtosecond pump−probe spectroscopy was carried out by Bigot and co-workers.[11] In contrast with thin film studies, they found a slower electron−electron relaxation (∼700 fs) and a slower rate of cooling of the electron gas to the lattice temperature.

Recently, we reported picosecond dynamics of colloidal gold nanoparticles of 30 nm diameter.[21] We found that subpicosecond pulsed laser excitation leads to the "bleach" of the surface plasmon band and induces a positive transient absorption at the

[⊗] Abstract published in *Advance ACS Abstracts,* April 1, 1997.

S1089-5647(96)02923-9 CCC: $14.00

wings of the "bleached" plasmon band. Both "bleach" and positive absorption were found to decay with lifetimes of 2.5 and >50 ps at low laser intensities. These observations were interpreted as follows: a rapid formation of a transient non-Fermi "hot" electron distribution within the colloidal particles on a time scale shorter than our time resolution occurs. The equilibration or relaxation of the "hot" electrons takes place through (a) electron−phonon scattering (2−3 ps) and (b) phonon−phonon relaxation (>50 ps).

In the present paper we extend our study of electron dynamics to smaller colloidal gold nanoparticles by choosing different gold samples containing particles with average diameters as small as 1.9 nm (∼200 Au atoms), whose structural and steady-state optical properties have been separately characterized.[22,23] To our knowledge, this is the first report on the ultrafast electron dynamics of metal structure bridging the cluster (<50 atoms, or subnanometer) and colloidal (>5 nm) regimes. A substantial difference in the spectral response of the nanoparticles with different sizes was observed. This spectral difference in the transient spectra of the gold particles with different sizes is explained in terms of electronic level quantization within small size particles. Also, we found that the lifetime of electron−phonon scattering is laser intensity (excitation density) dependent. This lifetime increases from 2.5 ps at low laser power to 5 ps at high laser intensity, which is explained by an increase in the heat capacity of electron gas as the temperature increases.

Experimental Section

The water solution of colloidal gold particles were prepared by the method of Turkevich et al.[24] which involves the reduction of $HAuCl_4$ by sodium citrate. The average particle radius was determined to be 15 ± 3 nm using TEM. The preparation and characterization of the passivated gold nanocrystals are described fully in the accompanying article. The two smaller diameter samples (1.9 and 2.6 nm) are passivated by $-SC_{12}H_{25}$ monolayers, whereas the largest (3.2 nm) is passivated by a short-chain, $-SC_6H_{13}$, monolayer. The size distribution of the particles is ±10% of the average size. The colloids of passivated gold nanocrystals were dissolved in toluene, and they have high photostability.[22]

The laser system is similar to that described previously.[25] Briefly, the laser system consists of a commercial Coherent Satori dye laser pumped by an Antares mode-locked YAG laser and amplified by regenerative amplifier. As a result, 300−400 fs pulses with a repetition rate of 10 Hz and energy of 700−1000 μJ at wavelengths between 595 and 615 nm were generated. The 595−615 nm pulse was mixed with residual fundamental radiation (1064 nm) of regenerative amplifier in KDP crystal in order to obtain radiation at 380−390 nm. The output energy in 380 nm typically is about 0.2 mJ.

The optical density of the samples used in the transient absorbance measurements was about 1.0 per 2 mm optical path length at the excitation wavelength. The transient spectroscopy setup was described previously.[25] The energy of the pump beam was about 0.05 mJ at 380 nm or 0.1−0.2 mJ at 600 nm. The reference beam had an energy of less than 50 nJ. The reference and probe beams were passed through a monochromator or polychromator and were detected by two photodiodes or a CCD detector (Princeton Instruments, EUV-1024, controller ST-130), respectively. Kinetics were analyzed by the least-squares method.

Results

As the steady-state UV−vis absorption spectrum of gold nanoparticles shows, there is no plasmon type band present in the sample with average particle size of 1.9 nm, but rather a onset to strong absorption starting at 1.7 eV (750 nm).[23] However, there is a weak plasmon band in the sample containing particles of 2.6 nm which has a maximum around 517 nm. The plasmon band maxima for 3.2 and 30 nm particles are at 522 and 530 nm, respectively. These spectra are shown in Figure 1. The absence of a plasmon band in small metallic particles is attributed to quantum-size effects which leads to the formation of quantized energy states, in contrast to band formation in larger particles, and it is discussed in the next section.

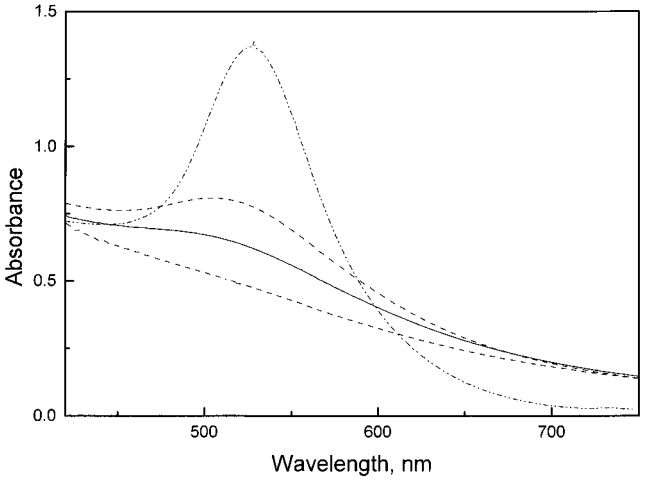

Figure 1. Absorption spectra of the gold nanoparticles of different size: 30 (dash-dot line), 3.2 (dash line), 2.6 (solid line), and 1.9 nm (lowest dash line).

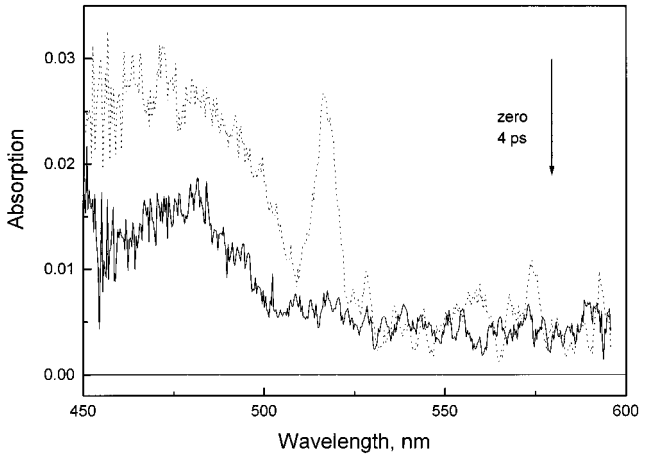

Figure 2. Transient absorption spectra of the 1.9 nm gold nanoparticles obtained immediately after excitation with 600 nm laser pulse (dot line) and at 4 ps delay (solid line).

The transient absorption data for particles of 1.9 nm size are shown in Figure 2. Immediately after the photoexcitation with a 600 nm laser pulse, a band around 470 nm is observed. It should be mentioned that in gold particles, unlike silver particles for example, the plasmon band maximum and the interband transition maximum are very close in energy, 2.35 and 2.45 eV, respectively.[26] The band at 470 nm is due to interband transition or due to thermal redistribution of electrons below the Fermi level. The 470 nm band cannot be associated with plasmon electrons, since these particles lack any plasmon band. As will be discussed later, similar absorption features at 470 nm were seen for gold nanoparticles of all sizes. This absorption decays to the base line within a few picoseconds without any changes in the spectral profile. The peak at 520 nm results from the Raman scattering of the solvent (toluene). This peak is not seen in other samples, probably because of higher

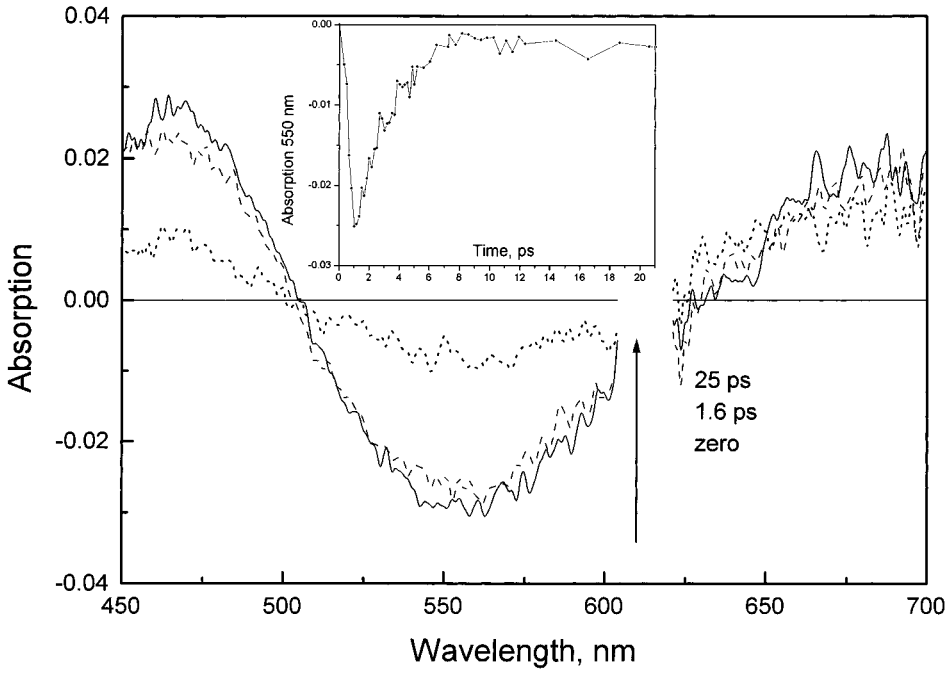

Figure 3. Transient absorption spectra of 2.6 nm nanoparticles of gold at different delay after excitation by laser pulse. Inset: kinetics of absorption changes measured at 550 nm.

TABLE 1: Energies of the Steady-State Plasmon Band Maximum, "Bleached" Plasmon Band after Laser Excitation, and Energy Splitting between Electronic States in Gold Nanoparticles of Different Size

diameter, nm	steady-state plasmon band, eV	laser-induced "bleach" of plasmon band, eV	energy spacing between electronic states, meV
1.9			60
2.6	2.42	2.25	20
3.2	2.39	2.29	10
30	2.36	2.35	0.001

excitation power used in the case of the smallest nanoparticles.

For 2.6 nm particles, photoexcitation with 600 nm, 350 fs laser pulses leads to the absorption changes shown in Figure 3. At time zero the positive absorption at 470 nm, similar to that of 1.9 nm particles, is seen. Also, a negative signal with a minimum around 555 nm and a positive feature with a maximum around 690 nm is observed. The minimum is due to the plasmon band "bleach", and the positive absorption, as was assigned previously[21] for the 30 nm particles, is due to absorption of "hot" electrons of the plasmon band. The dynamics of the plasmon band "bleach" recovery (Figure 3, inset) is biexponential, similar to that of large nanoparticles.[21] The lifetime of the fast component of this "bleach" decay was found to be 2−2.5 ps (inset in Figure 3), similar to that for 30 nm particles,[21] and it is discussed later in this paper. There is a considerable shift in the minimum of the plasmon band "bleach" and maximum of the steady-state plasmon absorption, as given in Table 1.

The transient spectra for 3.2 nm particles, obtained after excitation with subpicosecond laser pulse, are shown in Figure 4. The basic features of these absorption spectra are similar to that of the 2.6 nm particle: positive absorptions at 470 and 680 nm and a negative absorption with its maximum at 540 nm. The dynamics of this absorption is similar to the 2.6 nm gold particles with a slight shift in the minimum of the plasmon band "bleach" and maximum of the "hot" plasmon band absorption (Table 1).

The data for 30 nm gold particles were given previously[21] and showed spectral features (Figure 5) similar to those for

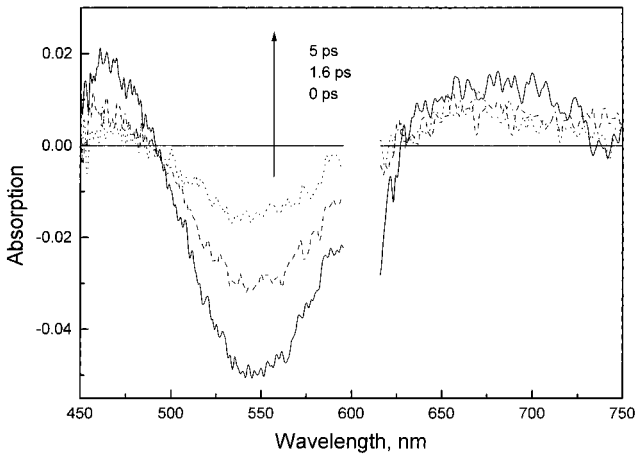

Figure 4. Transient absorption spectra of 3.2 nm gold nanoparticles at delays 0 (solid line), 1.6 (dash line), and 5 ps (dot line).

smaller size gold nanoparticles (with the exception of the 1.9 nm particles). However, the contribution of the plasmon band "bleach" relative to the positive absorption at 630 and 490 nm is much larger for 30 nm particles than that for 2.6 and 3.2 nm particles. The dynamics of the plasmon band "bleach" recovery has two components with lifetimes of 2.5 and >50 ps, as was shown previously,[21] and it is similar to that observed for 2.6 nanoparticles.

The kinetics of the plasmon band "bleach" recovery shows that as laser intensity increases, so does the lifetime of the fast component, going from 2.5 ps at low intensity to 5 ps at higher intensity (Figure 6). Moreover, the relative contribution of the slow component becomes larger by a factor of 3 at high laser intensities (Figure 6).

Discussion

Subpicosecond optical excitation leads to instantaneous changes in the conduction-electron distribution of a metal. This nonequilibrium distribution is expected to be rapidly thermalized, creating an equilibrium "hot" electron distribution around the Fermi level. During the thermalization process, the electron

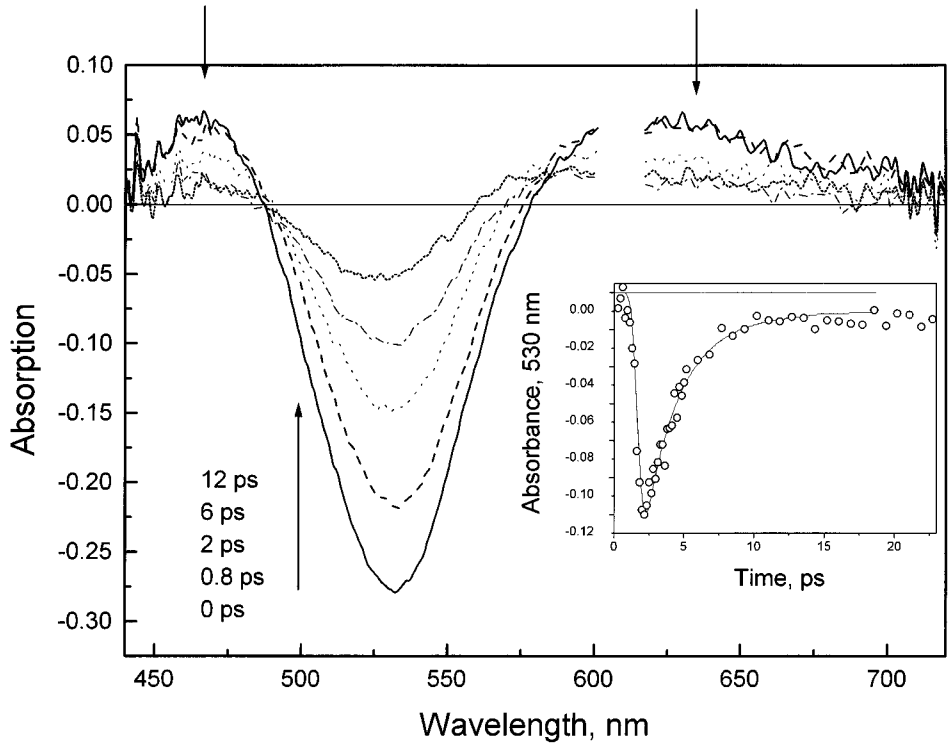

Figure 5. Transient absorption spectra of 30 nm gold nanoparticles measured at delays 0, 0.8, 2.0, 6.0, and 12 ps after excitation with 350 fs, 600 nm laser pulse. Arrows indicate the change of intensity with time. Inset: kinetics of the absorption changes at 530 nm, solid line is a fit with lifetimes of 2.5 and >50 ps.

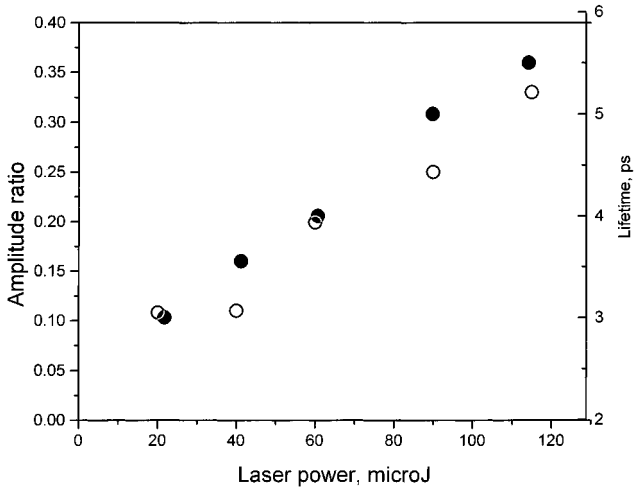

Figure 6. Ratio of the amplitudes of the slow to the fast component (closed circles, left scale) and lifetime of the fast component in the kinetics of the absorption changes at 530 nm for 30 nm gold nanoparticles (open circles, right scale) as a function of laser pulse intensity.

gas loses its energy and interacts with the lattice through electron−phonon scattering. After thermalization a new quasi-equilibrium at higher than the original temperature will be reached. In thin films of gold this process takes a few picoseconds and was extensively studied.[15−19] After the lattice is heated, a dissipation to the solvent occurs in a time scale of ~100 ps. The redistribution of electrons modifies the dielectric function. At the same time, the plasmon band intensity and its position depend on the dielectric function and reflect the dynamics of electronic equilibration and cooling. It indicates that absorption changes at the plasmon band region are associated with thermal electron relaxation.

The first question to be answered is the origin of the absorption changes found in the present study. A clear correlation between the amplitude of the "ground-state" plasmon band in different size gold nanoparticles with the laser-induced absorption changes suggests that the observed absorption changes are due to the plasmon band contribution for the particle size of 2.5−30 nm. However, as mentioned earlier, in gold the interband transition (2.45 eV) is close in energy to the plasmon band (2.35 eV), so the contribution of the two excitation channels is expected. In fact, absorption changes in 1.9 nm gold nanoparticles (Figure 1) are attributed to the transition from the d-band as these particles do not have surface plasmon absorption (see also ref 23).

The transmission changes of the gold nanoparticles could be described in analogy to that used for the gold thin film,[19] with the origin of the surface plasmon band taken into account. Transmission of the thin film[19] at low levels of excitation may be written as

$$\Delta T/T = (\delta \ln T/\delta\epsilon_1)\Delta\epsilon_1 + (\delta \ln T/\delta\epsilon_2)\Delta\epsilon_2 \qquad (1)$$

where ϵ_1 and ϵ_2 are real and imaginary parts of gold's dielectric response. The changes of the real and imaginary part of dielectric function could be calculated through the changes of electron distribution as was suggested by Rossei et al.[27] The changes in ϵ_2 can be calculated using the constant matrix element approximation as

$$\epsilon_2 = 1/(h\omega)^2 \int D(E,h\omega)\, \Delta\rho(E)\, \mathrm{d}E \qquad (2)$$

where $D(E,h\omega)$ is the so-called "joint density of states" with respect to the energy of the final state (E). The D function is calculated assuming a parabolic band structure for the conductive band and a much flatter d-band around the L point of the Brilloiun zone, as was suggested by Rossie et al.[27] The change in the real part of dielectric constant is calculated through Kramers−Kronig relationship. This part of the calculation is similar to that given by Fujimoto et al.[13] for gold thin films. We note here that the observed shape of the transient signal for

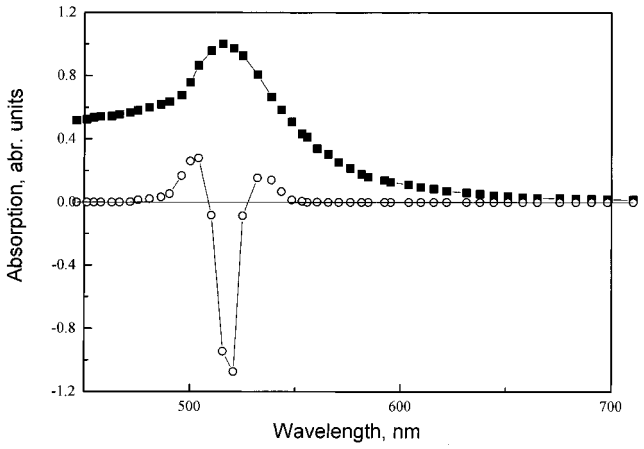

Figure 7. Shape of the plasmon band (filled squares) and transient absorption changes after laser excitation (open circles) calculated on the basis of eqs 1−3.

thin film[13] and that measured in the present paper for gold nanoparticles are very similar (negative absorption in the middle with two positive wings at higher and lower energies around negative absorption). However, there is a difference in the positions of these peaks as well as their relative intensities. The signal measured in thin films[13] (center peak is at 510 nm) is due to the interband transition alone, whereas the main contribution in the case of nanoparticles is expected to be from the plasmon band (maximum at 530 nm for the 30 nm particles). For the contribution of the plasmon band we use the expression for absorption given by Mie theory:[26]

$$1 - T = (18\pi NV{n_0}^3/\lambda)\epsilon_2/((\epsilon_1 + 2{n_0}^2)^2 + {\epsilon_2}^2) \qquad (3)$$

where N is the particle number density, V is their volume, and n_0 is the refractive index of the medium. The absorption peak occurs whenever $(\epsilon_1 + 2n_0^2) = 0$. The absorption bandwidth and plasmon damping are directly related to the imaginary part of the dielectric function of gold ϵ_2. Expression 3 reproduces the absorption shape of the large size gold nanoparticles (Figure 7) reasonably well, despite the fact that this is the dipole approximation. Higher terms in the Mie theory are neglected, since they are insignificant within the size regime that we are concerned.[26] Expression 3 combined with eq 1 reproduces the absorption changes associated with the plasmon due to temperature changes. Calculation of the absorption changes based on this approach gives good correlation with the experiment (Figure 7): the minimum due to "bleaching" at 530 nm and two positive wings are reproduced. However, there is a difference in the calculated "bleach" and positive transient bands signal widths as compared to the experimental results. The theoretical calculations were performed in the limit of the weak perturbation, when the change in electronic gas temperature was equal to 1 K. The energy of the excitation in the experiment (2.04 eV) was high, which corresponds to an approximately 1000 K temperature change. We attribute the difference between calculated and experimental spectra to the different perturbation limits.

The above description of the absorption changes is based on the assumption that the fast component of the plasmon band "bleach" recovery is due to the hot electron−phonon scattering. However, as it was suggested recently by Bigot et al.[11] for metallic copper nanoparticles, the contribution of electron−electron interaction and energy relaxation to the lattice on the picosecond time scale must be also considered. The change of the symmetry of the plasmon band change around the Fermi level with time was observed in this experiment. As seen in Figure 8 (replot of Figure 5), where absorption changes of the 30 nm gold nanoparticles at different times are normalized, no substantial difference in the band shape within the time range of 6 ps could be seen. There is a small time-dependent shift of the crosspoint of absorption changes with zero base line (shown in the inset), which probably reflects the lowering of electron gas equilibrium temperature leading to the lattice heating. However, for time delays as long as 12 ps (Figure 7), there is a noticeable difference in the band shape as compared to that at short time delay. We attribute this to the contribution of electron−phonon interaction with phonons of the solvent or scattering of excited electrons by surface defects.

There is a substantial difference in the position of the plasmon band "bleach" for nanoparticles of different sizes (Figures 2−5) as compared to the position of their steady-state absorption (Figure 1). Because the maximum of the transient signal is located around the Fermi level, the changes in dielectric constant are the largest. The electron density function D[19] is nearly a constant around the Fermi level. Therefore, in order to explain the difference in the plasmon band absorption maximum for different size gold nanoparticles and position of the plasmon band "bleach" observed in our experiment, we have to assume that the electronic density of states is different in nanoparticles of different sizes. Moreover, in small size particles, the distribution of electrons around the Fermi level may be different from "normal" Fermi distribution. This leads us to the conclusion that these size-dependent effects are mainly due to the changes in the electron density function. Obviously, the larger the spacing between electronic states in a small size particle, the larger is the shift observed in the steady-state position of the plasmon band and its "bleach" in the transient spectrum. The spacing between adjusted electronic levels are generally expressed as $\delta \sim 2E_F/N$, where E_F is the Fermi energy and N is the number of atoms. It is obvious that $\delta \sim 1/d^3$, where d is the diameter of the particle. The smallest particle, where d is equal to 1.9 nm, contains about $N = 200$ atoms. This means that δ is ∼0.1 eV, which is higher than kT at room temperature. For 2.6 nm particles, $N = 600$ atoms; the δ is about 0.02 eV, which is close to kT at room temperature. Table 1 shows the shift between steady-state absorption of the plasmon and the position of its "bleach" after laser excitation. There is some correlation between this shift and δ for particles of different sizes; i.e., the shift becomes minimum as particle size increases. Also, a critical size of 5 nm is estimated from this correlation, when the size-dependent shift disappears. (The shift becomes smaller than the measurement's accuracy.)

The ratio of the plasmon band "bleach" to the amplitude of the positive wings in transient spectra, as shown in Figures 1−5, decreases as size of the nanoparticles becomes smaller. Figure 9 shows the size dependence of this ratio. One can assume that there is a linear relationship between this ratio and the particles with smaller than 5 nm diameters, and it becomes independent of size at larger than 5 nm. Again, 5 nm could be considered as the critical size above which a transition from the "small particle" to the "large particle" regimes takes place.

For the small particles the conservation of the wave vector k and specificity transition around the L point of the Brillouin zone for the interband transition is not necessary anymore. This may lead to the broadening of the plasmon band and transient wings in absorption changes or even its breakup into discrete transitions.[23] These features are best observed at low temperatures, as has recently been shown for ∼1 nm alkali-metal clusters in beams.[28]

The increase of the excitation laser power may lead to multiphoton absorption by the gold nanoparticles, and subse-

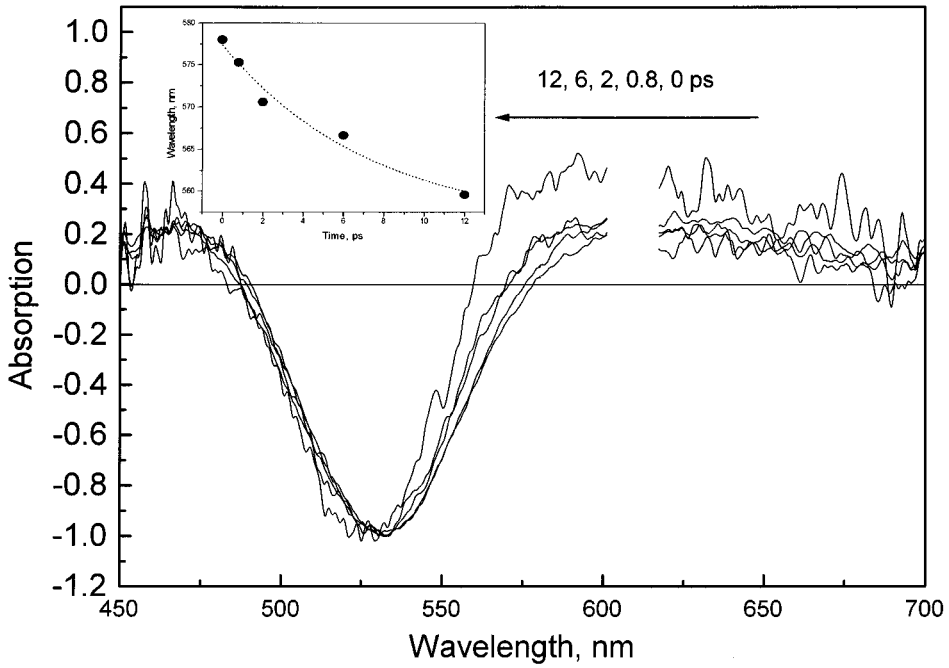

Figure 8. Absorption changes of the 30 nm gold nanoparticles at different delay times normalized on their peak intensity. The arrow indicates the direction of the changes with time increase.

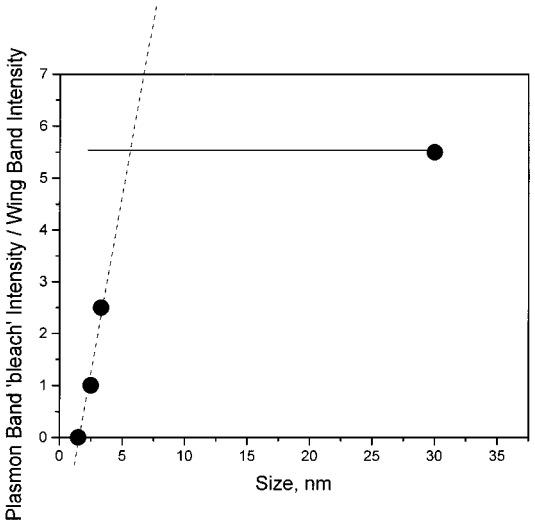

Figure 9. Dependence of the amplitudes ratio of plasmon band "bleach" to the positive wing as a function of the particle's size. The lines indicate the linear relationship and saturation range.

quently, it will lead to higher electronic temperature and more heating of the lattice. The phonon−phonon scattering is the rate-limiting step in the cooling of gold nanoparticles. An increase of the electron gas temperature will lead to a higher lattice temperature, which increases the relative contribution of the slow component in the "bleach" recovery kinetics of the gold nanoparticles. Because the heat capacities of the lattice and electrons are well separated, electronic gas and lattice could be treated independently, interacting through the electron−phonon coupling constant. That is a limit for the two-temperature model (TTM).[3] At low excitation intensities, when temperature changes are small, electron gas heat capacity and electron−phonon interaction may remain constant. At high levels of excitation, however, that is not the case. Therefore, the increase of the lifetime of electron−phonon interaction observed with the laser excitation power increase is consistent with the temperature dependence of the electronic heat capacity. Furthermore, at higher temperatures the saturation of the change in electronic occupancy takes place. This may also lead to an increase in the lifetime of thermal relaxation. The effect of the increase of the transient reflectivity lifetime in thin films of gold was observed previously after excitation with high-power femtosecond laser pulses.[18]

Conclusion

The temporal dynamics of the laser-induced absorption changes in gold nanoparticles for samples with average particle size of 1.9, 2.6, 3.2, and 30 nm was studied. These absorption changes originate from plasmon band changes (except for 1.9 nm particles) with laser-induced thermal redistribution of the conductive electrons (or the d-electrons) in the gold nanoparticles. Theoretical calculations based on this approach quantitatively reproduce the shape of the transient absorption. The difference in the transient signal for particles of different size is ascribed to the changes in the density of electronic states. The power dependence of the kinetics of the electron cooling process is consistent with the temperature dependence of the electronic heat capacity.

Acknowledgment. The Office of Naval Research (Grant N00014-95-1-0306) is acknowledged for its financial support of this project.

References and Notes

(1) Henglein, A.; Mulvaney, P. *Ber. Bunsen-Ges. Phys. Chem.* **1994**, *98*, 180.

(2) Sun, C.-K.; Vallee, F.; Acioli, L. H.; Ippen, E. P.; Fujimoto, J. G. *Phys. Rev. B* **1993**, *48*, 12365.

(3) Groenneveld, R. H. M.; Spirk, R.; Lagedijk, A. *Phys. Rev. B* **1995**, *51*, 11433.

(4) Perenboom, J. A.; Wyder, P.; Meier, P. *Phys. Rep.* **1981**, *78*, 173.

(5) Bloemer, M. J.; Haus, J. W.; Ashley, P. R. *J. Opt. Soc. Am. B* **1990**, *7*, 790.

(6) Roberti, T. W.; Smith, B. A.; Zhang, J. Z. *J. Chem. Phys.* **1995**, *102*, 3860.

(7) Heilweil, E. J.; Hochstrasser, R. M. *J. Chem. Phys.* **1985**, *82*, 4762.

(8) Doremus, R. H. *J. Chem. Phys.* **1964**, *40*, 2389.

(9) Papavassiliou, G. C. *Prog. Solid State Chem.* **1980**, *12*, 185.

(10) Maxwell-Garnett, J. C. *Philos. Trans. R. Soc. London* **1904**, *203*, 385.
(11) Bigot, J.-Y.; Merle, J.-C.; Cregut, O.; Daunois, A. *Phys. Rev. Lett.* **1995**, *75*, 4702.
(12) Mie, G. *Ann. Phys. (Leipzig)* **1908**, *25*, 377.
(13) Fujimoto, J. G.; Liu, J. M.; Ippen, E. P.; Bloembergen, N. *Phys. Rev. Lett.* **1984**, *53*, 1837.
(14) Fann, W. S.; Storz, R.; Tom, H. W. K.; Boker, J. *Phys. Rev. Lett.* **1992**, *68*, 2834.
(15) Brorson, S. D.; Fujimoto, J. G.; Ippen, E. P. *Phys. Rev. Lett.* **1987**, *59*, 1962.
(16) Elsayed-Ali, H. E.; Juhasz, T.; Smith, G. O.; Bron, W. E. *Phys. Rev. B* **1991**, *43*, 19914.
(17) Wright, O. B. *Phys. Rev. B* **1994**, *49*, 9985.
(18) Schoenlein, R. W.; Lin, W. Z.; Fujimoto, J. G.; Eesley, G. L. *Phys. Rev. Lett.* **1987**, *58*, 1680.
(19) Sun, C.-K.; Vallee, F.; Acioli, L. H.; Ippen, E. P.; Fujimoto, J. G. *Phys. Rev. B* **1994**, *50*, 15337.
(20) Fann, W. S.; Strorz, R; Tom, H. W. K.; Boker, J. *Phys. Rev. B* **1992**, *46*, 13592.
(21) Ahmadi, T.; Logunov, S. L.; El-Sayed, M. A. *J. Phys. Chem.* **1996**, *100*, 8053.
(22) (a) Whetten, R. L.; Khoury, J. T.; Alvarez, M. M.; Murthy, S.; Vezmar, I.; Wang, Z. L.; Stephens, P. W.; Cleveland, C. L.; Luedtke, W. D.; Landman, U. *Adv. Mater.* **1996**, *5*, 428. (b) *Chemical Physics of Fullerenes 5 and 10 Years Later*; Andreoni, W., Ed.; Kluwer: Dordrecht, 1996; p 475.
(23) Accompanying paper: Alvarez, M. M.; Khoury, J. T.; Schaaf, T. G.; Shafigullin, M. N.; Veznar, I.; Whetten, R. L.; Alvarez, M. M. *J. Phys. Chem. B* **1997**, *101*, 3706.
(24) Enustun, B. V.; Turkevich, J. *J. Am. Chem. Soc.* **1963**, *85*, 3317.
(25) Logunov, S. L.; El-Sayed, M. A.; Song, L.; Lanyi, J. K. *J. Phys. Chem.* **1996**, *100*, 2391.
(26) Kreibig, U.; Vollmer, M. *Optical Properties of Metal Clusters*; Springer: Berlin, 1995.
(27) Rosei, R.; Antonangeli, F.; Grassano, U. M. *Surf. Sci.* **1973**, *37*, 689.
(28) Ellert, C.; Schmidt, M.; Schmitt, C.; Reines, T.; Haberland, H. *Phys. Rev. Lett.* **1995**, *75*, 1731.